©Daniyan et al.

THE EFFECT OF BITTER HONEY AGAINST CEREBRAL MALARIA-INDUCED INFLAMMASOME CELL DEATH: NETWORK PHARMACOLOGY-BASED *IN SILICO* EVALUATION

M.O. Daniyan[1]*, O.B. Adeoye[2], E. Osirim[1,3], I.D. Asiyanbola[1,4]

[1]Faculty of Pharmacy, Obafemi Awolowo University,
Ile-Ife, Osun State, Nigeria; *e-mail: mdaniyan@oauife.edu.ng
[2]Benjamin Carson (Snr.) School of Basic Medical Sciences, Babcock University,
Ilishan-Remo, Ogun State, Nigeria
[3]Faculty of Basic Medical Science, Redeemer's University, Ede, Osun State, Nigeria
[4]College of Health Sciences, Osun State University, Osogbo, Osun State, Nigeria

Cerebral malaria (CM) is a fatal complication of *Plasmodium falciparum* infection. The biological and physiological links between CM, inflammation, and inflammasome, point to the complexity of its pathology. Resistance to available and affordable drugs, worsening economic crisis, and urgent need for integration of orthodox with traditional/alternative medicine, actualized the search for sustainable pharmacotherapy. Previous works from our team on the medicinal properties of bitter honey have established botanical and bioactive markers, inhibitory effects on pancreatic alpha-amylase activity, and anti-dyslipidemia, cardio-protective, and ameliorative effects on hepatorenal damage in streptozotocin-induced diabetic rats. In this study, we have identified bitter honey (BH) derived phytochemicals using gas chromatography coupled with mass spectrometry (GC-MS), and 9 targets from genes associated with CM, inflammation, inflammasome, and BH phytochemicals. Network analysis revealed significant functional and physical interactions among these targets and NOD-, LRR-, and pyrin domain-containing protein 3 (NLRP3). Molecular docking of bitter honey-derived phytochemicals against these targets identified 3 most promising phytochemical candidates for further experimental validation. Based on these results, we predict that bitter honey may aid in the suppression of CM-mediated inflammasome cell death via its interactions with these targets.

Key words: cerebral malaria; inflammation; inflammasome; bitter honey; phytochemicals; network pharmacology

DOI: 10.18097/PBMC20247006442

INTRODUCTION

The global prevalence of malaria in 2022 was estimated at 249 million cases, resulting in 5 million cases above that of 2021, with associated 608,000 deaths, and the most vulnerable group was children under the age of five years old [1]. The African region continues to bear the bulk of malaria cases and deaths, with Nigeria, the most populous country, accounting for 27% of malaria morbidity and 31% mortality [1]. The gains of the widely advocated artemisinin-based combination therapies (ACTs), including high efficacy, short duration of treatment which improves compliance, and a globally reduced rate of morbidity and mortality, have been threatened due to the emergence of resistance to artemisinin [1, 2]. The reported incidence of malaria parasite decreased sensitivity to the ACT drugs is of great concern and this could be disastrous for malaria global control.

Cerebral malaria (CM), a fatal complicating nervous syndrome resulting from *Plasmodium falciparum* infection, is known to be associated with permanent disabilities and/or deaths, especially among children [3]. The emergence of CM occurs in only about 1% of *P. falciparum* infections; however the mortally rate can reach 15–25% [4]. Survivors experience acute or long-lasting physical disability and neurological syndrome post-infection treatment [4, 5]. These appearances vary in children and adults and depend on the commencement and severity of the infection and associated symptoms, which include coma, status epilepticus, focal sequelae, hyperactivity, impaired movement, inappropriate vision, and speech. Better management of CM and associated neurological alterations can only be achieved with precise and early diagnosis, resulting from improved knowledge of the disease pathology and specificity of the infection [4, 5]. The intent of managing CM is to primarily decrease mortality and improve the quality of life thereby curtailing the neurological syndromes that follow even after effective use of antimalarial. Hence, there is a need to continue the search for new pharmacotherapy that would not only terminate the disease advancement but also reverse the pathological proceedings in the brain [4]. More details on the CM pathology and associated neurological syndromes have been presented in [5].

Natural products have played critical roles in the management of malaria, and medicinal plants have been sources of very effective antimalarial drugs including quinine and artemisinin. With the renewed interest in the integration of traditional with orthodox medicine, the need for a better understanding of the pharmacology of natural products is inevitable.

Honey is one of the mostly used natural products for varieties of beneficial health purposes [6]. In general, good evidence exists that honey possesses antioxidant, anti-inflammatory, anti-hyperglycaemia, etc properties [6, 7]. However, it should be noted that the medicinal properties of honey largely depend on the sources of the nectars used by the honey bees [8]. Bitter honey is a variety of honey that is cultivated predominantly from the nectar of plants which conserve distinct bitter bioactive compounds [8]. Our earlier works on the medicinal properties of bitter honey, have been able to establish botanical and bioactive markers, inhibitory effects on pancreatic alpha-amylase activity, and anti-dyslipidaemia, cardio-protective, and ameliorative effects on hepatorenal damage in streptozotocin-induced diabetic rats [8–11]. Therefore, bitter honey may have potential usefulness in ameliorating neurological syndrome and CM-mediated inflammasome-induced cell death.

It is a well-known fact that several highly effective drugs act on several targets rather than just one target. Today, by utilizing network pharmacology-based computational methods to integrate and analyze large-scale data from diverse sources, it is possible to identify the underlying biological mechanisms of drug action and potential drug targets. Network pharmacology is an interdisciplinary field of research that aims to understand the multifaceted interactions between biological systems and drugs at a molecular level [12]. It has been used to investigate the molecular mechanisms of disease and to identify new drug targets, drug combinations, repurposing existing drugs, and improving the safety and efficacy of drugs for the treatment of complex diseases [12, 13].

We have earlier presented a detailed review, highlighting some of the biochemical and molecular players in the CM pathology, with special emphasis on the functional interplay between inflammatory mediators, neurotransmitters, and molecular chaperones of human and plasmodial origins [5]. In this study, we have identified phytochemicals associated with bitter honey, and targets associated with CM, inflammation, inflammasome, and bitter honey phytochemicals. Finally, these targets were analyzed using a Network Pharmacology approach integrated with molecular docking.

MATERIAL AND METHODS

The workflow for the network pharmacology integrated molecular docking approach adopted in this study is presented in Figure 1.

Phytochemical Profiling of Bitter Honey by GC-MS

Phytochemical profiling of bitter honey samples was conducted using Agilent 8860 gas chromatography (GC) coupled with a 5977B mass spectrometry detector (MSD), fitted with an HP5 capillary column coated with 5% phenyl methyl siloxane (30 m length × 0.32 mm diameter × 0.25 μm film thickness), and equipped with GC/MSD Chemstation (MassHunter) suite of software (Agilent Technologies, USA). The protocol for the GC-MS phytochemical profiling was adapted from previous reports [14, 15]. Briefly, 1 μl of the samples were injected using an Agilent 8860 Automatic Liquid Sampler (ALS) and in split-less mode, injection temperature of 250°C. The inlet pressure was set at 10.296 psi and a total flow of 45.2 ml/min. Purge flow to the split vent was set at 40 ml/min at 0.5 min. Helium was used as a carrier gas of 99.9% with a constant column flow of 1 ml/minute. The GC oven temperature was initially programmed at 80°C (2.0 min) and then ramped at 30°C/min to 320°C (5 min). The MSD temperature was set at 300°C with Hydrogen : Air flow at 20 ml/min : 30 ml/min. Determination of the levels of GC amenable phytochemicals in the sample was carried out using GC-MS by operating MSD in scan mode. After the instrument was prepared for analysis, a sequence of samples was created on the Masshunter GC-MS Acquisition software. The sequence was then analyzed and the obtained data was subsequently analyzed on the Agilent Data Analysis software (version 12.1). The 3D structures and SMILES representations of the phytochemicals were obtained from the PubChem database [16]. A local database of the phytochemicals was generated in sdf format from the 3D structure using Discovery Studio Visualizer [17].

Retriever and Generation of Consensus Genes

Genes associated with CM, inflammation, and inflammasome were retrieved from the Open Targets and Human Genes Database [18, 19]. Duplicate entries were removed from each set of genes and stored in Microsoft Excel for subsequent use. The prediction of interacting genes for each BH phytochemical was performed using Swiss Target Prediction [20]. The predicted genes for all the phytochemicals were combined, and duplicate entries were also removed. The online Venn Diagram [21] was used to generate consensus genes.

Network Analysis of the Consensus Genes

Network analysis, including gene ontology and pathways enrichment analysis [22], of the final consensus genes was performed using STRING and ShinyGO (version 0.80) online servers [23, 24], with further analysis and hub genes identification and ranking using Cytoscape [25]. A protein-protein interaction (PPI) network was obtained from STRING using a full STRING Network, with a medium confidence score of 0.4000 and an FDR (false discovery rate) stringency of 0.5. Also, the setting did not allow the automatic inclusion of additional proteins apart from those supplied as query targets. The PPI was retrieved from STRING via the ShinyGO 0.80 web interface,

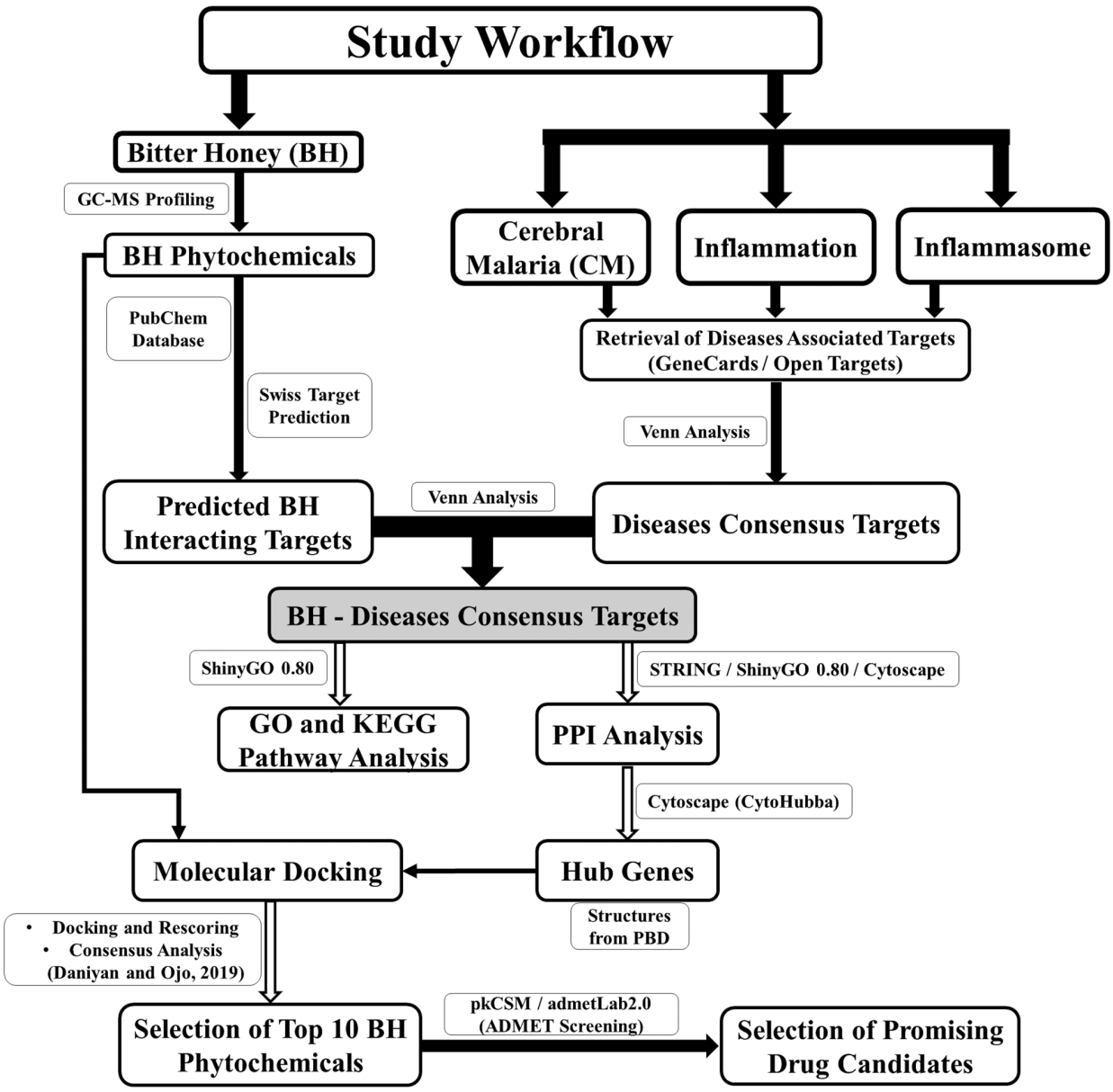

Figure 1. Network Pharmacology integrated Molecular docking workflow. PPI, Protein-Protein Interaction; GO, Gene Ontology; KEGG, Kyoto Encyclopedia of Genes and Genomes; BH, Bitter Honey; ADMET, Absorption, Distribution, Metabolism, Excretion, and Toxicity. The pkCSM, admetLab2.0, STRING, ShinyGO, Swiss Target Prediction, Venn, Gene Cards, KEGG, and Open Targets are online resources. Cytoscape is a software with the capacity to interact with online resources, such as the STRING database.

and the PPI edges indicate both functional and physical protein associations. To further assess the functional roles of these genes, NLRP3, one of the most studied genes in inflammasome, was included, to determine potential functional relationship with the consensus genes, and serve as functional control.

Molecular Docking of BH Phytochemicals Into the Consensus Genes

Representative protein structures for all identified targets were retrieved from the protein databank [26] and were prepared for docking as earlier described [27]. These included: ADORA2A (PDB: 3PWH), C5AR1 (PDB: 8HK5), FCGR1A (PDB: 4X4M), ITGB2 (PDB: 3K72), NOS2 (PDB: 4NOS), PTGS2 (PDB: 3HS5), STAT3 (PDB: 6NJS), VDR (PDB: 5V39), VEGFA (PDBs: 4KZN and 6ZFL), and added NLRP3 (PDB: 8ETR). Briefly, the downloaded structures were first checked and corrected for missing atoms using a Swiss-pdb viewer [28]. Thereafter, using the VEGA ZZ platform [29], water and hydrogen were removed, and the coordinates were normalized and checked for charge distribution. The binding site residues were mapped around co-crystallized ligands with a radius of 5 Å, followed by the removal of the co-crystallized ligands to create the needed space for docking, as implemented in VEGA ZZ [29]. The BH phytochemicals were screened against these targets using Autodock Vina [30], while their respective

co-crystallized ligands served as controls. The generated poses from Autodock Vina were rescored using PLANTS, XScore, and NNSCORE [29, 31, 32] and the results were subjected to consensus analysis as earlier described [27]. The generated scores from the screening were ranked, and the ranked scores were analyzed to determine the phytochemical(s) with the highest potential for functional interaction with multiple targets.

In Silico ADMET Screening of Bitter Honey Phytochemicals

The sub-database in sdf and SMILES representations of the top 10 phytochemicals with the highest potential for functional interactions with multiple targets were generated from the local database of BH phytochemicals using ADSV [17]. The ADMET screening was performed using pkCSM and admetlab 2.0 online servers [33, 34].

RESULTS

Comparative Analysis of Target Genes Associated with BH Phytochemicals

Comparative analysis was performed with genes predicted to be associated with CM, inflammation, and inflammasome. Venn analysis has shown that a substantial part of the genes predicted to be associated with inflammasome (1948 genes) and CM (391) are subsets of inflammation-associated genes (13646) (Supplementary Materials Fig. S1A and S1B). Further analysis revealed association of CM-inflammasome consensus genes (134) with inflammation (Supplementary Materials Fig. S1C and S1D). Meanwhile, the BH chemical profiling using GC-MS produced 28 phytochemicals (Supplementary Materials Tables S4 and S5). The quantitative analysis of these phytochemicals as reported by the GC-MS is given in Supplementary Materials Table S7. A high percentage of genes associated with BH (329) were found to be involved in inflammation (303 genes) (Supplementary Materials Fig. S2B), a subset of which is associated with CM (28) (Supplementary Materials Fig. S2A and S2D) and inflammasome (66) (Supplementary Materials Fig. S2C and S2F). The least association is BH-CM-Inflammasome, which produced 9 consensus genes (Supplementary Materials Fig. S2E). It is interesting to note that the consensus analysis of CM-Inflammation-Inflammasome (CM-II) with BH-associated genes also produced 9 genes (Fig. 2A), similar to BH-CM-Inflammasome consensus (Supplementary Materials Fig. S2E and S3C). Also, all the BH-associated genes (329) are associated with inflammation, of which 66 genes are also associated with inflammasome (Fig. 2D). However, in the context of CM and CM-inflammation-associated BH genes, 28 genes were identified, of which 9 genes showed association with CM, inflammation, and inflammasome. Therefore, this analysis revealed 9 BH-associated targets that are also involved in the pathogenic mechanisms of CM, inflammation, and inflammasome. These included ADORA2A, C5AR1, FCGR1A, ITGB2, NOS2, PTGS2, STAT3, VDR, and VEGFA.

Protein-Protein Interaction Analysis

Protein-protein interaction (PPI) analysis provides an opportunity to assess the functional relationship between identified targets. For better understanding of the functional roles of these targets, NLRP3, one of the most studied inflammasome proteins [36–38], was included as a functional control to ascertain the potential functional interplay with the identified targets. Comparative analysis of the functional interactions among these targets with and without NLRP3 was performed. The results of the PPI analysis of the 9 targets alone and with NLRP3 are shown in Figure 3. The PPI analysis identified 38 (p = 1.05e-11) (Fig. 3B) and 29 (p = 2.64e-08) (Fig. 3A) functional and physical protein interactions with and without NLRP3 respectively. This suggests that the presence of NLRP3 does increase the prospects of functional interactions of the identified targets.

Gene Ontology and Enrichment Analysis

A total of 162 and 146 enriched biological functions (BF) were identified with the target genes with or without NLRP3 included in the analysis respectively (Supplementary Materials Table S1). Of these, 134 were similar, and though numerically different in some associated BF, the percentage of occurrences of the identified targets in these BF were not significantly different with or without NLRP3. Analysis of the association of identified targets with BF (Table 1 upper panel) has shown that all the 9 targets are implicated in 8 BF, namely, positive regulation of the cellular process, regulation of catalytic activity, regulation of the cellular metabolic process, regulation of nitrogen compound metabolic process, regulation of the primary metabolic process, response to organic substance, and signal transduction (Supplementary Materials Table S1). Interestingly, NLRP3 was also found to be associated with these BFs (Supplementary Materials Table S1). In addition, NLRP3 was also found in association with a high percentage of BF found to be associated with 8, 7, 6, and 5 of the identified targets (Table 1 upper panel), suggesting a potential functional relationship between NLRP3 and the target genes.

Similarly, a total of 96 KEGG pathways were found in association with the target with or without NLRP3 (Supplementary Materials Table S2). Of these, only five pathways showed association with NLRP3 and one or two of the targets, from which only one (pertussis) was found within the top 20 pathways

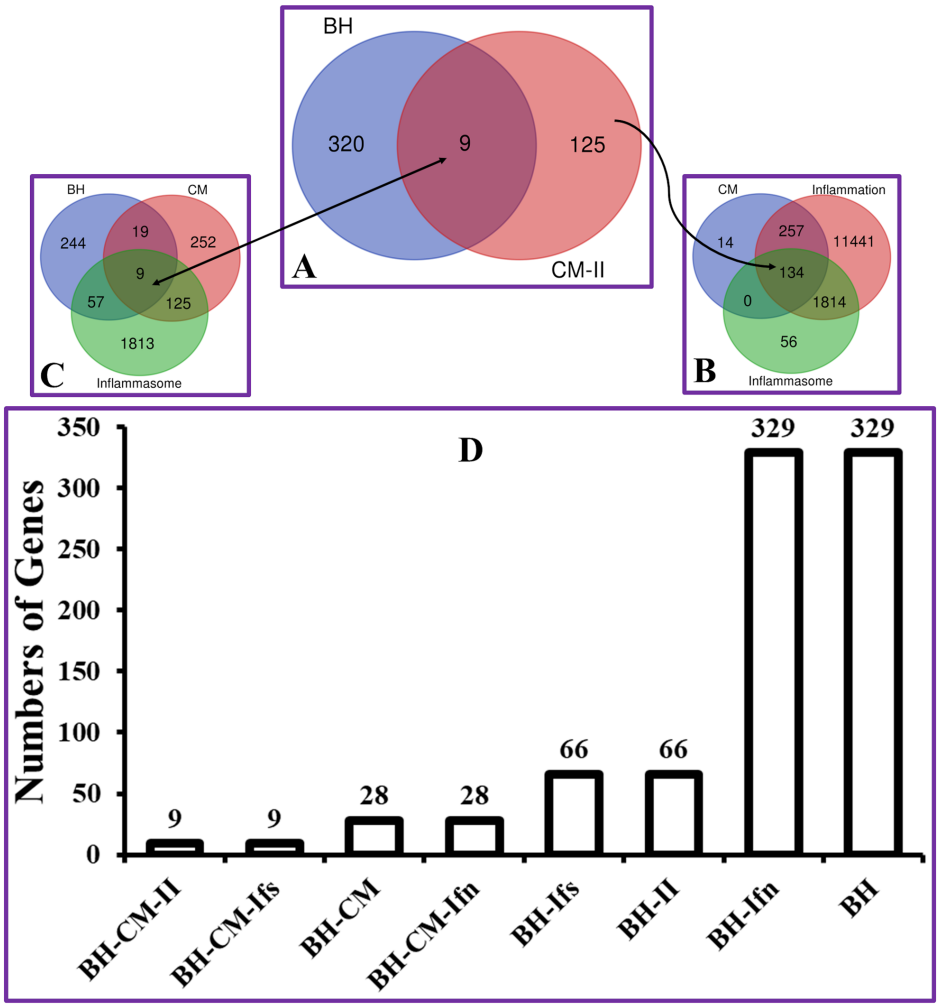

Figure 2. Comparative analysis of the BH-associated genes with CM-associated Inflammation and Inflammasome genes. BH, Bitter Honey; CM, Cerebral malaria, Ifs, Inflammasome; Ifn, Inflammation; II, Inflammasome-Inflammation. Venn diagrams show a consensus of (**A**) BH-CM-II, (**B**) CM-Ifn-II, and (**C**) BH-CM-II. (**D**) is the bar plot of BH-associated genes in consensus with CM, inflammation, and inflammasome genes. The bar plot was generated on Microsoft Excel, and images were prepared using Microsoft PowerPoint and GIMP 2.10.14 [35].

Table 1. Analysis of genes association with Biological Functions and KEGG Pathways with or without NLRP3

Consensus Genes Association with Biological Functions			
Number of Consensus Genes	**Number of Associated BF**	**Number of Associated BF with NLRP3 Association**	**% NLRP3 Association**
9	8	8	100.00
8	14	11	78.57
7	13	8	61.54
6	15	8	53.33
5	17	10	58.82
4	23	8	34.78
3	21	4	19.05
2	23	0	0
Consensus Genes Association with KEGG Pathways			
Number of Consensus Genes	**Number of Associated KEGG Pathways**	**Number of Associated KEGG Pathways with NLRP3 Association**	**% NLRP3 Association**
4	3	0	0
3	9	0	0
2	20	2	10.00
1	64	3	4.69
0	0	6	0

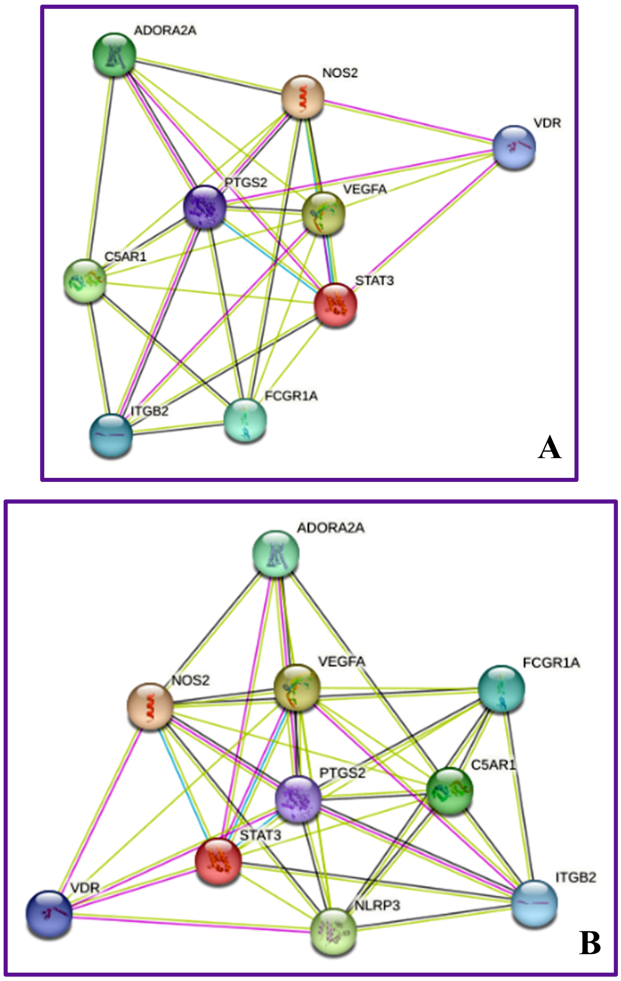

Figure 3. Protein-protein interaction (PPI) analysis of the identified targets alone (**A**) and with NLRP3 (**B**). Nodes, representing each protein, are represented as spherical shapes and filled nodes indicate that the 3D structure is known or predicted. Lines represent interactions predicted from experimentally determined data (purple), protein homology (light blue), co-expression (black), gene neighborhood (green), and gene co-expression (blue). Images were generated from ShinyGO-String and prepared using Microsoft PowerPoint and GIMP 2.10.14 [35]. The color version of the figure is available in the electronic version of the article.

(Table 1 lower panel, Table 2, and Supplementary Materials Table S2). The additional six pathways were only associated with NLRP3 (Supplementary Materials Table S2). The lack of significant association of NLRP3 with the targets in the KEGG pathways suggests a differential functional association in most of the identified KEGG pathways. Analysis of the frequency of gene association revealed that 4 was the highest number of genes and was found in association with three disease pathways, namely, Leishmaniasis, Tuberculosis, and pathways in Cancer (Tables 1, 2, and Supplementary Materials Table S2). This is followed by 9, 20, and 64 pathways in association with 3, 2, and 1 pathway(s), respectively (Table 1 lower panel, Table 2, and Supplementary Materials Table S2).

Therefore, it does appear that the presence of NLRP3 does not alter the target gene association in the KEGG pathways. This is further confirmed by the enrichment functional charts and hierarchical clustering trees (Supplementary Materials Fig. S4). The analysis showed that except for the replacement of Rheumatoid arthritis with COVID-19, the inclusion of NLRP3 did not significantly alter the KEGG enrichment pathways. However, fold enrichment and the number of genes associated with each pathway were altered. Also, the trees help to appreciate the correlation among significant pathways (Supplementary Materials Fig. S4A) by clustering together the pathways that share similar genes. The hierarchical clustering revealed more significant *p*-values with tuberculosis and leishmaniasis.

Furthermore, the 12 scoring functions of the cytoHubba plugin in Cytoscape [25] were used to rank the genes. The consensus analysis of cytoHubba ranked scores identified several hub genes (ranked parenthesis) below. Without NLRP3 the genes were ranked as STAT3 (1), ITGB2 (2), FCGR1A (3), C5AR1 (4), PTGS2 (5), and NOS2 (6). In the case of analysis with NLRP3, the genes were ranked in the following order: STAT3 (1), PTGS2 (2), C5AR1 (3), FCGR1A (4), NLRP3 (5), ITGB2 (6), and NOS2 (7). The results showed that the presence of NLRP3 did alter the PPI among the target genes as earlier stated.

Screening and Identification of the Most Promising BH Phytochemicals

We performed an *in silico* screening of the functional interaction of BH phytochemicals against the identified targets and NLRP3 to identify promising phytochemicals from BH with the potential to alter CM-mediated inflammasome cell death. Small molecule co-crystalized ligands associated with all the downloaded proteins from PDB served as control(s) for each protein. The resulting energy of binding from virtual screening is presented in Supplementary Materials Table S4. Following consensus analysis of docking scores, for each screening against a specific receptor site of the downloaded target proteins, the phytochemicals were ranked from lowest/best (ranked 1) to the highest/failed (ranked 29 — BH phytochemicals and the co-crystalized control) (Supplementary Materials Table S5). Consensus analysis of the rank scores was performed for the entire set of proteins (target proteins and NLRP3), as earlier described [27]. Our analysis revealed that of the control co-crystalized ligands, three ranked 1, one ranked 2, two ranked 4, four ranked between 12 and 16, and others ranked above 22 (Supplementary Materials Table S5), suggesting that most of the BH phytochemicals interacted with the proteins better than their co-crystalized ligands. The relative positions of the top 10 BH phytochemicals and control in a total of 29 ligands (28 BH phytochemicals and

Table 2. KEGG enrichment pathways and associated consensus genes

S/No.	KEGG Pathways	Genes	Enrichment	
			Fold	FDR
1	Leishmaniasis	FCGR1A, ITGB2, NOS2, PTGS2	133.81	1.37E-06
2	VEGF signaling pathway	PTGS2, VEGFA	86.18	0.001753
3	Staphylococcus aureus infection	FCGR1A, ITGB2, C5AR1	81.14	0.000181
4	Acute myeloid leukemia	FCGR1A, STAT3	75.89	0.002101
5	HIF-1 signaling pathway	NOS2, STAT3, VEGFA	69.97	0.000212
6	Pancreatic cancer	STAT3, VEGFA	66.90	0.002365
7	Pertussis*	ITGB2, NOS2, NLRP3	66.90	0.002365
8	EGFR tyrosine kinase inhibitor resistance	STAT3, VEGFA	64.36	0.002405
9	Complement and coagulation cascades	ITGB2, C5AR1	59.82	0.002628
10	Tuberculosis	FCGR1A, ITGB2, NOS2, VDR	56.81	2.17E-05
11	Small cell lung cancer	NOS2, PTGS2	55.27	0.002770
12	Rheumatoid arthritis	ITGB2, VEGFA	55.27	0.002770
13	MicroRNAs in cancer	PTGS2, STAT3, VEGFA	47.37	0.000534
14	Neutrophil extracellular trap formation	FCGR1A, ITGB2, C5AR1	40.35	0.000553
15	Kaposi sarcoma-associated herpesvirus infection	PTGS2, STAT3, VEGFA	39.31	0.000553
16	Chemical carcinogenesis-receptor activation	STAT3, VDR, VEGFA	38.72	0.000553
17	Rap1 signaling pathway	ADORA2A, ITGB2, VEGFA	36.32	0.000602
18	Human cytomegalovirus infection	PTGS2, STAT3, VEGFA	34.05	0.000663
19	Calcium signaling pathway	ADORA2A, NOS2, VEGFA	31.78	0.000746
20	Pathways in cancer	NOS2, PTGS2, STAT3, VEGFA	19.19	0.000534

* KEGG Pathway that is associated with NLRP3.

Table 3. Rank scores of the top 10 bitter honey phytochemicals following docking against target proteins

PHYTOCHEMICALS	ADORA2A	C5AR1	FCGR1A	ITGB2	NLRP3	NOS2	PTGS2	STAT3	VDR	VEGFA	Average	
											Score	Rank
Ergosta-5,22-dien-3-ol	1	1	1	3	1	2	3	2	6	2	2.2	1
Friedelan-3-one	4	2	2	1	2	4	1	3	7	1	2.6	2
Alpha-Amyrin	7	3	3	1	3	3	1	4	13	3	4.3	3
Aciphyllene	3	4	6	7	6	6	4	5	11	4	5.6	4
(E)-2-bromobutyloxychalcone	5	5	4	17	5	5	5	11	2	8	6.7	5
Beta-Guaiene	6	9	7	4	10	8	6	9	4	5	6.8	6
5-Acetamido-4,7-dioxo-4,7-dihydrobenzofurazan	15	10	5	4	8	11	8	6	7	6	8.0	7
Octahydronaphthalene	9	5	8	7	11	10	7	11	5	9	8.2	8
aR-Turmerone	7	7	9	9	8	9	9	14	10	7	8.9	9
1H-Cyclopropa[a]naphthalene	10	7	10	14	7	7	10	11	14	10	10.0	10
Control (Co-crystalized ligand)	2	25	19	12	4	1	25	1	1	24	—	—

1 co-crystalized ligand as control) are shown in Table 3. The 2D representations of the structures of the top 10 BH-derived phytochemicals are provided in Figure 4, and those of the representative co-crystallized ligands are presented in Supplementary Materials Figure S3. When taken together, the consensus scoring analysis revealed that the BH phytochemicals have the potential to perform functional interaction across all the target proteins, especially with the top 3 phytochemicals (Table 3).

Furthermore, we checked the identified top 10 phytochemicals for ADMET properties using online pkCSM and admetlab2.0 servers [33, 34]. Our analysis revealed that the top 10 phytochemicals showed

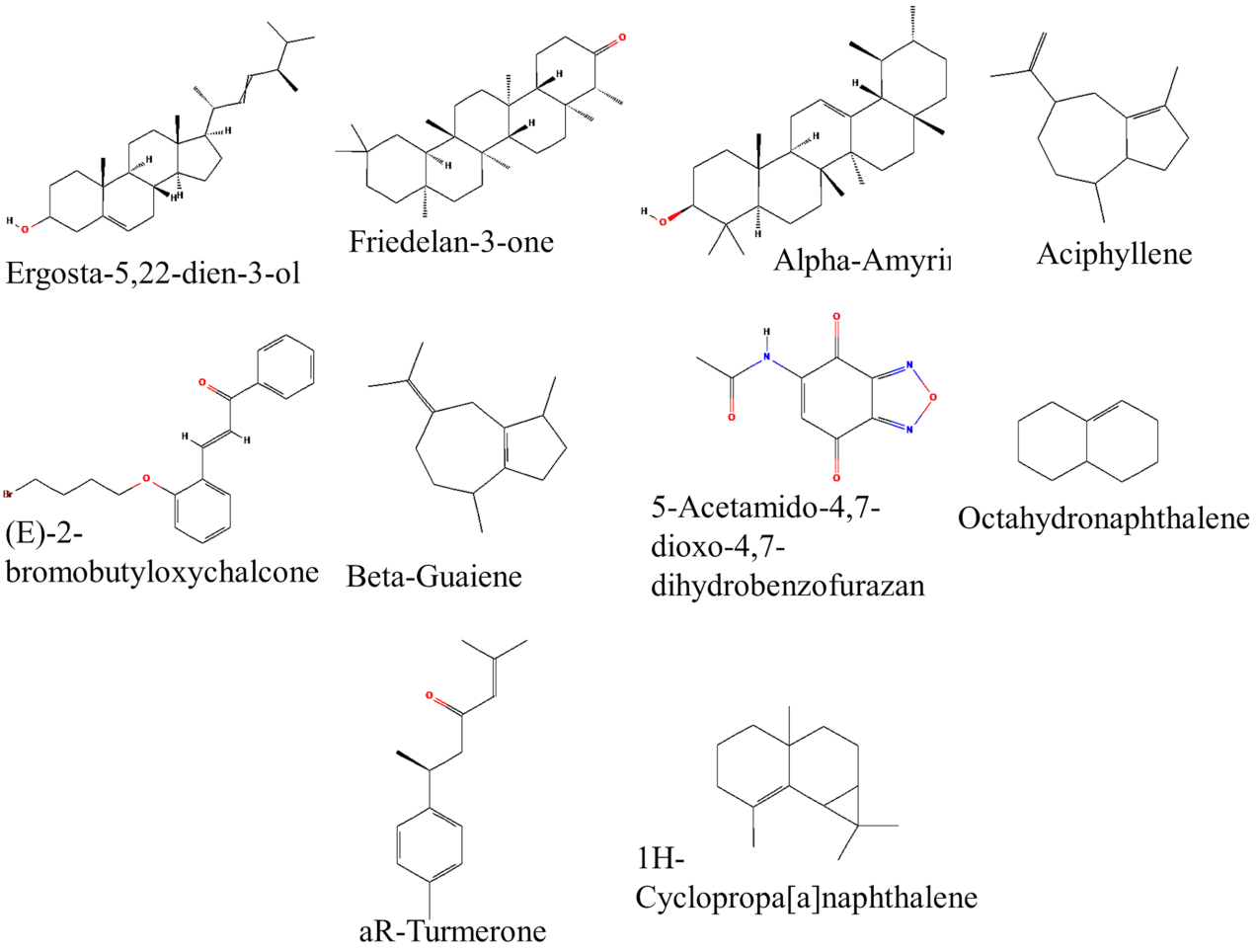

Figure 4. 2D Structures of the top 10 BH-derived phytochemicals exhibiting functional interactions with identified target proteins and NLRP3.

good ADMET properties (Table 4 and Supplementary Materials Table S6). Essentially, the top 3 compounds revealed a high probability for intestinal absorption, CNS and BBB permeability, and very low potential for toxicity (Table 4), and shared similar structural backbones (Fig. 4), indicating added advantages that can be explored for improved activities against inflammasome mediated cell death in CM. Interestingly, the top 3 phytochemicals ranked mostly within 1 and 3 in their interaction with the hub genes, further confirmed their potential multi-targets functional interactions.

In addition, the interaction scheme for the best interacting phytochemical and control co-crystallized ligand for each of the target proteins and NLRP3 are presented in Figure 5. The interaction analysis revealed that apart from VDR which showed preference interaction with (E)-2-bromobutyloxychalcone, the best interactions with other target proteins and NLRP3 were mainly with the three promising BH phytochemicals: Ergosta-5,22-dien-3-ol, Friedelan-3-one, and Alpha-Amyrin. Of these three, Ergosta-5,22-dien-3-ol ranked top with six targets. In addition to being commercially available, quantitatively, GC-MS revealed 3.18%, 13.55%, and 1.08% abundance of Ergosta-5,22-dien-3-ol, Friedelan-3-one, and Alpha-Amyrin in the bitter honey respectively (Supplementary Materials Table S7). Though showing interactions with residues within the mapped receptor site, and with some similar residues when compared to control co-crystallized ligand, and hydrogen bond interactions with some key residues, suggesting stability of interaction, the functional relevance of these interactions needs to be further explored.

DISCUSSION

Inflammasomes are intricate protein assemblies situated within the cytosol. The initiation of these assemblies occurs upon the identification of stimuli that are linked to infection or stress [39]. It is a key component of the innate immune system and is primarily involved in detecting intracellular pathogens, as well as endogenous danger signals, known as damage-associated molecular patterns (DAMPs) [40]. The activation of the inflammasome can be initiated by a wide variety of microbial pathogens, and its primary function is to contribute to the host's defense mechanism by promptly

Table 4. Selected ADMET properties of the top 10 bitter honey phytochemicals

Phytochemicals	Lipinski	Excretion	Pgn		Permeability					Toxicity			Rank
			INH	SUB	Caco2	I#	Skin	CNS	BBB	DILI	Ames	C*	
Ergosta-5,22-dien-3-ol	YES	Moderate	0.064	0.001	1.213	94.515	-2.819	-1.719	0.857	0.114	0.030	0.047	1
Friedelan-3-one	YES	High	0.086	0	1.236	97.452	-2.722	-1.471	0.484	0.022	0.038	0.012	2
Alpha-Amyrin	YES	High	0.181	0	1.327	94.156	-2.811	-1.809	0.762	0.012	0.011	0.017	3
Aciphyllene	YES	Moderate	0.200	0	1.408	94.084	-1.518	-2.182	0.884	0.394	0.015	0.602	4
(E)-2-bromobutyloxychalcone	YES	Low	0.991	0.001	1.288	93.522	-2.654	-1.382	0.109	0.745	0.653	0.744	5
Beta-Guaiene	YES	Moderate	0.922	0.001	1.416	94.704	-1.596	-2.149	0.377	0.729	0.011	0.583	6
5-Acetamido-4,7-dioxo-4,7-dihydrobenzofurazan	YES	Low	0.247	0.001	0.133	78.303	-2.88	-3.199	0.982	0.992	0.950	0.943	7
Octahydronaphthalene	YES	High	0.002	0	1.415	94.484	-1.434	-1.858	0.890	0.045	0.011	0.770	8
aR-Turmerone	YES	Moderate	0.766	0.002	1.667	95.352	-1.377	-1.707	0.202	0.259	0.015	0.475	9
1H-Cyclopropa[a]naphthalene	YES	Moderate	0.024	0.008	1.591	95.848	-1.728	-1.292	0.845	0.879	0.873	0.881	10

Pgn is P-glycoproteins INH is Inhibitor; SUB is Substrate; I# is Intestinal; CNS is Central Nervous System BBB is Blood Brain Barrier; DILI is Drug-induced Liver Injury; C* is Carcinogenicity. Pgn (INH and SUB), BBB, and Toxicity (DILI, Ames, and C*) are rated on a scale of probability of 0 (NO) to 1 (YES). Caco2 > 0.90, Intestinal > 90%, skin < -2.50, and CNS > -2 are regarded as great.

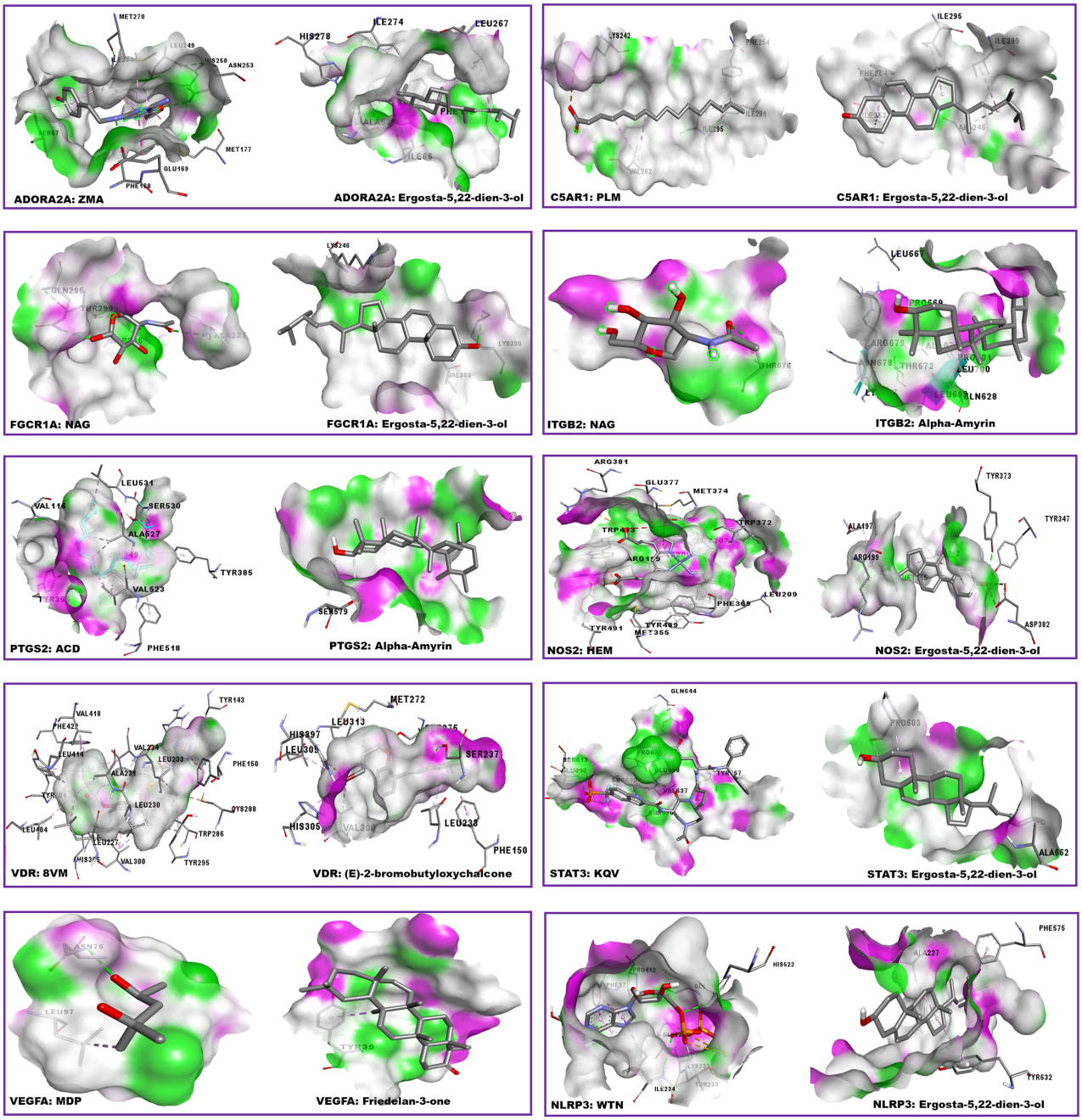

Figure 5. Representative interaction analysis of the best most promising phytochemicals and co-crystallized ligands with selected proteins. Images are labelled as protein : ligand. Ligands and interacting protein residues are represented as sticks, coloured by element. Hydrogen bonds are shown as surface with shades of purple and green representing hydrogen donor and acceptor respectively. Hydrogen bond interactions are indicated as green broken lines. Images were generated using ADSV, arranged on Microsoft PowerPoint, and prepared using GIMP 2.10.14 [35]. The color version of the figure is available in the electronic version of the article.

initiating inflammatory responses and restricting pathogen replication [41]. Recent research has provided evidence suggesting that the inflammasome, in addition to its role in immune defense against pathogens, plays a pivotal role in the regulation of inflammatory responses and cellular apoptosis [42]. There are several types of inflammasomes identified, but the most extensively studied and well-characterized inflammasome is the NOD-like receptor family, pyrin domain-containing 3 (NLRP3) inflammasome. Aberrant activation of the NLRP3 inflammasome, in particular, has been implicated in several neurological conditions including cerebral malaria [36, 38]. Therefore, NLRP3 is a critical factor in CM-mediated inflammasome, and any direct or indirect interaction with small molecules may have profound effects on the NLRP3 inflammasome pathways.

In CM, factors released by *P. falciparum* parasites, as well as host-derived molecules, can activate the NLRP3 inflammasome [36]. As it has been earlier

reported [5], this is undoubtedly a complex interplay of many factors, including neurotransmitters, molecular chaperones, and inflammatory and inflammasome mediators. In this study, we have identified 9 target genes with links to inflammation, inflammasome, and CM, and having potential for functional and physical interactions using a combination of comparative genes analysis and network pharmacology. The PPI analysis revealed significant (p = 2.64e-08) functional and physical interactions among these targets. We further explored the potential of these genes to functionally interact with NLRP3, a well-studied inflammasome protein. The increase in significant (p = 1.05e-11) functional and physical interactions from 29 to 38 is a clear demonstration of the potential functional interplay between the 9 consensus proteins and NLRP3, as well as the potential of the identified targets to modulate NLRP3 activities. This is further supported by the gene ontology and enrichment analysis, which revealed that NLRP3 was also found to be in association together with these genes in several biological functions (BF). The identified genes are: ADORA2A, C5AR1, FCGR1A, ITGB2, NOS2, PTGS2, STAT3, VEGFA, and VDR. However, Cytoscape revealed that six of them could be considered as hub genes (C5AR1, FCGR1A, ITGB2, NOS2, PTGS2, STAT3). Available evidence show that these genes have potential for functional interplay with NLRP3, performed active roles in inflammation, inflammasome, and CM, and may serve as drug targets in CM and associated inflammasome pathways [36, 43]. Cell death is a fundamental biological process that occurs in various physiological and pathological contexts, and several reports have provided insights into the mechanisms of cell death in CM, with clear links to inflammatory and inflammasome mediators [43]. This study has shown that a high percentage of the genes associated with CM and inflammasome are also associated with inflammation.

In light of the above potentials of the identified targets, we further explored the functional interaction of the 9 CM-Inflammasome linked targets with BH-derived phytochemicals. *In silico* screening of the BH-derived phytochemicals against these targets and NLRP3 performed using molecular docking and ADMET, identified 10 most promising BH-derived phytochemicals with significantly higher functional interaction when compared to their respective co-crystalized ligands. However, with the added advantages of high probability for intestinal absorption, CNS and BBB permeability, and very low potential for toxicity (Table 4 and Supplementary Materials Table S6), the top 3 BH phytochemicals can be explored further as lead molecules against CM and associated inflammasome-mediated cell death. These BH phytochemicals (Ergosta-5,22-dien-3-ol, Friedelan-3-one, and Alpha-Amyrin) which shared some levels of structural similarities, also showed very strong functional interaction with the six hub targets (Fig. 5). While the functional relevance of these interactions needs further exploration, the observed interactions with a higher or equivalent number of key residues within the receptor site in most of the interacting partners, as compared to the control co-crystallized ligand, confirm the potential of these BH phytochemicals as promising drug candidates. Meanwhile, though the overall inference from our ADMET analysis of the BH phytochemicals (Table 4 and Supplementary Materials Table S6) shows that BH is to a large extent safe, the potential inhibitory effects of the individual phytochemicals on P-glycoprotein I or II, and hERG, as well as serving as inhibitor and/or substrates of some key cytochrome P450 enzymes, may be an indication of possible side effects and/or drug-drug interactions. This, however, will need further evaluation.

CONCLUSIONS

We have performed a comparative analysis of genes associated with CM, inflammation, inflammasome, and BH-derived phytochemicals, using a Venn diagram, and identified 9 consensus genes. Network analysis revealed significant functional and physical interactions among these targets alone and with NLRP3. These targets are implicated in many biological functions, with clear link to inflammation, inflammasome, and directly or indirectly with CM, and to a larger extent with NLRP3 inflammasome pathways, suggesting potential for functional interplay. Further analysis with Cytoscape revealed six hub genes. The *in silico* screening of bitter honey-derived phytochemicals against these targets identified 3 most promising candidates for further experimental validation. Based on these results, we predict that the identified targets could serve as potential drug targets, and the bitter honey may aid in the suppression of CM-mediated inflammasome cell death via its interactions with these targets.

FUNDING

This research did not receive any specific grant from funding agencies in the public, commercial, or not-for-profit sectors.

COMPLIANCE WITH ETHICAL STANDARDS

This article does not contain any research involving humans or the use of animals as objects.

CONFLICT OF INTEREST

The authors declare no conflicts of interest.

Supplementary materials are available in the electronic version at the journal site (pbmc.ibmc.msk.ru).

REFERENCES

1. World Health Organization (2023) World malaria report 2023. from: https://www.who.int/publications-detail-redirect/9789240086173
2. *Dondorp A.M., Nosten F., Yi P., Das D., Phyo A.P., Tarning J., Lwin K.M., Ariey F., Hanpithakpong W., Lee S.J., Ringwald P., Silamut K., Imwong M., Chotivanich K., Lim P., Herdman T., An S.S., Yeung S., Singhasivanon P., Day N.P., Lindegardh N., Socheat D., White N.J.* (2009) Artemisinin resistance in *Plasmodium falciparum* malaria. N. Engl. J. Med., **361**(5), 455–467. DOI: 10.1056/NEJMOA0808859
3. *Desruisseaux M.S., Machado F.S., Weiss L.M., Tanowitz H.B., Golightly L.M.* (2010) Cerebral malaria: A vasculopathy. Am. J. Pathol., **176**, 1075–1078. DOI: 10.2353/ajpath.2010.091090
4. *Shikani H.J., Freeman B.D., Lisanti M.P., Weiss L.M., Tanowitz H.B., Desruisseaux M.S.* (2012) Cerebral malaria: We have come a long way. Am. J. Pathol., **181**, 1484–1492. DOI: 10.1016/j.ajpath.2012.08.010
5. *Daniyan M.O., Fisusi F.A., Adeoye O.B.* (2022) Neurotransmitters and molecular chaperones interactions in cerebral malaria: Is there a missing link? Front. Mol. Biosci., **9**, 965569. DOI: 10.3389/fmolb.2022.965569
6. *Palma-Morales M., Huertas J.R., Rodríguez-Pérez C.* (2023) A comprehensive review of the effect of honey on human health. Nutrients, **15**(13), 3056. DOI: 10.3390/nu15133056
7. *Floris I., Pusceddu M., Satta A.* (2021) The Sardinian bitter honey: From ancient healing use to recent findings. Antioxidants, **10**(4), 506. DOI: 10.3390/antiox10040506
8. *Adeoye B.O., Iyanda A.A., Daniyan M.O., Adeoye A.D., Oyerinde A.M., Olatinwo G.O.* (2022) Botanical and bio-active markers of Nigerian bitter honey. Trop. J. Nat. Prod. Res., **6**(11), 1848–1853. DOI: 10.26538/tjnpr/v6i11.17
9. *Adeoye O.B., Iyanda A.A., Daniyan M.O., Adeoye D.A., Olajide O.L., Akinnawo O.O., Olajide O.L., Akinnawo O.O., Adetunji A.O., Osundina B.O., Olatinwo O.M.* (2023) Anti-dyslipidaemia and cardio-protective effects of Nigerian bitter honey in streptozotocin induced diabetic rats. Univers. J. Pharm. Res., **8**(2), 10–18. DOI: 10.22270/ujpr.v8i2.920
10. *Adeoye O.B., Ayobola I.A., Daniyan M.O., Ekundina V.O., Adeoye D.A., Abijo Z.A., Akin-Akanbi F.B.* (2022) Ameliorative effects of Nigerian bitter honey on streptozotocin-induced hepatorenal damage in Wistar rats. Journal of Krishna Institute of Medical Sciences University, **11**(1), 65–76.
11. *Adeoye B.O., Iyanda A.A., Oyerinde A.M., Oyeleke I.O., Fadeyi B.O.* (2022) Inhibitory effects of Nigerian sweet and bitter honey on pancreatic alpha amylase activity. Nigerian J. Nutr. Sci., **43**(2), 19–24.
12. *Li X., Wei S., Niu S., Ma X., Li H., Jing M., Zhao Y.* (2022) Network pharmacology prediction and molecular docking-based strategy to explore the potential mechanism of Huanglian Jiedu Decoction against sepsis. Comput. Biol. Med., **144**, 105389. DOI: 10.1016/j.compbiomed.2022.105389
13. *Dai W., Chen H.-Y., Chen C.Y.-C.* (2018) A network pharmacology-based approach to investigate the novel TCM formula against Huntington's disease and validated by support vector machine model. Evid. Based Complement Alternat. Med., **2018**, 6020197. DOI: 10.1155/2018/6020197
14. *Joshna K., Gopal V., Kavitha B.* (2022) Analysis of bitter honey using gas chromatography and tandem mass spectrometry. Bioinformation, **18**(3), 196–199. DOI: 10.6026/97320630018196
15. *Castell A., Arroyo-Manzanares N., Guerrero-Núñez Y., Campillo N., Viñas P.* (2023) Headspace with gas chromatography-mass spectrometry for the use of volatile organic compound profile in botanical origin authentication of honey. Molecules, **28**(11), 4297. DOI: 10.3390/molecules28114297
16. *Kim S., Chen J., Cheng T., Gindulyte A., He J., He S., Li Q., Shoemaker B.A., Thiessen P.A., Yu B., Zaslavsky L., Zhang J., Bolton E.E.* (2018) PubChem 2019 update: Improved access to chemical data. Nucleic Acids Res., **47**(D1), D1102–D1109. DOI: 10.1093/nar/gky1033
17. Dassault Systèmes BIOVIA (2015) Discovery studio modelling environment, Release 4.5, San Diego: Dassault Systèmes.
18. *Stelzer G., Rosen N., Plaschkes I., Zimmerman S., Twik M., Fishilevich S., Stein T.I., Nudel R., Lieder I., Mazor Y., Kaplan S., Dahary D., Warshawsky D., Guan-Golan Y., Kohn A., Rappaport N., Safran M., Lancet D.* (2016) The GeneCards suite: From gene data mining to disease genome sequence analyses. Curr. Protoc. Bioinformatics, **54**, 1.30.1-1.30.33. DOI: 10.1002/cpbi.5
19. *Koscielny G., An P., Carvalho-Silva D., Cham J.A., Fumis L., Gasparyan R., Hasan S., Karamanis N., Maguire M., Papa E., Pierleoni A., Pignatelli M., Platt T., Rowland F., Wankar P., Bento A.P., Burdett T., Fabregat A., Forbes S., Gaulton A., Gonzalez C.Y., Hermjakob H., Hersey A., Jupe S., Kafkas Ş., Keays M., Leroy C., Lopez F.J., Magarinos M.P., Malone J., McEntyre J., Munoz-Pomer Fuentes A., O'Donovan C., Papatheodorou I., Parkinson H., Palka B., Paschall J., Petryszak R., Pratanwanich N., Sarntivijal S., Saunders G., Sidiropoulos K., Smith T., Sondka Z., Stegle O., Tang Y.A., Turner E., Vaughan B., Vrousgou O., Watkins X., Martin M.J., Sanseau P., Vamathevan J., Birney E., Barrett J., Dunham I.* (2017) Open Targets: A platform for therapeutic target identification and validation. Nucleic Acids Res., **45**(D1), D985-D994. DOI: 10.1093/nar/gkw1055
20. *Daina A., Michielin O., Zoete V.* (2019) SwissTargetPrediction: Updated data and new features for efficient prediction of protein targets of small molecules. Nucleic Acids Res., **47**(W1), W357–W364. DOI: 10.1093/nar/gkz382
21 Draw Venn Diagram. https://bioinformatics.psb.ugent.be/webtools/Venn/
22 *Gupta M.K., Gouda G., Selvaraj S., Donde R., Dash G.K., Ramakrishna V., Behera L.* (2021) Gene Ontology and Pathway Enrichment Analysis. In: Bioinformatics in Rice Research: Theories and Techniques (Gupta, M.K., Behera, L., eds.), pp. 257–279. Springer, Singapore. DOI: 10.1007/978-981-16-3993-7_12
23. *Ge S.X., Jung D., Yao R.* (2020) ShinyGO: A graphical gene-set enrichment tool for animals and plants. Bioinformatics, **36**(8), 2628–2629. DOI: 10.1093/bioinformatics/btz931
24. *Szklarczyk D., Gable A.L., Lyon D., Junge A., Wyder S., Huerta-Cepas J., Simonovic M., Doncheva N.T., Morris J.H., Bork P., Jensen L.J., Mering C.V.* (2019) STRING v11: Protein-protein association networks with increased coverage, supporting functional discovery in genome-wide experimental datasets. Nucleic Acids Res., **47**(D1), D607–D613. DOI: 10.1093/nar/gky1131
25 *Shannon P., Markiel A., Ozier O., Baliga N.S., Wang J.T., Ramage D., Amin N., Schwikowski B., Ideker T.* (2003) Cytoscape: A software environment for integrated models of biomolecular interaction networks. Genome Res., **13**(11), 2498–2504. DOI: 10.1101/gr.1239303

26. *Burley S.K., Bhikadiya C., Bi C., Bittrich S., Chao H., Chen L., Craig P.A., Crichlow G.V., Dalenberg K., Duarte J.M., Dutta S., Fayazi M., Feng Z., Flatt J.W., Ganesan S., Ghosh S., Goodsell D.S., Green R.K., Guranovic V., Henry J., Hudson B.P., Khokhriakov I., Lawson C.L., Liang Y., Lowe R., Peisach E., Persikova I., Piehl D.W., Rose Y., Sali A., Segura J., Sekharan M., Shao C., Vallat B., Voigt M., Webb B., Westbrook J.D., Whetstone S., Young J.Y., Zalevsky A., Zardecki C.* (2023) RCSB protein data bank (RCSB.org): Delivery of experimentally-determined PDB structures alongside one million computed structure models of proteins from artificial intelligence/machine learning. Nucleic Acids Res., **51**(D1), D488–D508. DOI: 10.1093/nar/gkac1077
27. *Daniyan M.O., Ojo O.T.* (2019) *In silico* identification and evaluation of potential interaction of *Azadirachta indica* phytochemicals with *Plasmodium falciparum* heat shock protein 90. J. Mol. Graph. Model., **87**, 144–164. DOI: 10.1016/j.jmgm.2018.11.017
28. *Johansson M.U., Zoete V., Michielin O.. Guex N.* (2012) Defining and searching for structural motifs using DeepView/Swiss-PdbViewer. BMC Bioinformatics, **13**, 173. DOI: 10.1186/1471-2105-13-173
29. *Pedretti A., Villa L., Vistoli G.* (2002) VEGA: A versatile program to convert, handle and visualize molecular structure on Windows-based PCs. J. Mol. Graph. Model., **21**(1), 47–49. DOI: 10.1016/s1093-3263(02)00123-7
30. *Trott O., Olson A.J.* (2010) AutoDock Vina: Improving the speed and accuracy of docking with new scoring function, efficient optimization and multithreading. J. Comput. Chem., **31**(2), 455–461. DOI: 10.1002/jcc.21334
31. *Korb O., Stützle T., Exner T.E.* (2006) PLANTS: Application of Ant Colony Optimization to Structure-Based Drug Design. In: Ant Colony Optimization and Swarm Intelligence (Dorigo M., Gambardella L.M., Birattari M., Martinoli A., Poli R., Stützle, T., eds.), pp. 247–258. Springer, Berlin, Heidelberg. DOI: 10.1007/11839088_22
32. *Durrant J.D., McCammon J.A.* (2011) NNScore 2.0: A neural-network receptor-ligand scoring function. J. Chem. Inf. Model., **51**, 2897–2903. DOI: 10.1021/ci2003889
33. *Pires D.E.V., Blundell T.L., Ascher D.B.* (2015) pkCSM: Predicting small-molecule pharmacokinetic and toxicity properties using graph-based signatures. J. Med. Chem., **58**(9), 4066–4072. DOI: 10.1021/acs.jmedchem.5b00104
34. *Xiong G., Wu Z., Yi J., Fu L., Yang Z., Hsieh C., Yin M., Zeng X., Wu C., Lu A., Chen X., Hou T., Cao D.* (2021) ADMETlab 2.0: An integrated online platform for accurate and comprehensive predictions of ADMET properties. Nucleic Acids Res., **49**(W1), W5–W14. DOI: 10.1093/nar/gkab255
35. The GIMP Development Team (2019) GIMP. The GNU Image Manipulation Program
36. *Ataide M.A., Andrade W.A., Zamboni D.S., Wang D., Souza M.dC., Franklin B.S., Elian S., Martins F.S., Pereira D., Reed G., Fitzgerald K.A., Golenbock D.T., Gazzinelli R.T.* (2014) Malaria-induced NLRP12/NLRP3-dependent caspase-1 activation mediates inflammation and hypersensitivity to bacterial superinfection. PLOS Pathog., **10**(1), e1003885. DOI: 10.1371/journal.ppat.1003885
37. *Blevins H.M., Xu Y., Biby S., Zhang S.* (2022) The NLRP3 inflammasome pathway: A review of mechanisms and inhibitors for the treatment of inflammatory diseases. Front. Aging Neurosci., **14**, 879021. DOI: 10.3389/fnagi.2022.879021
38. *Chiarini A., Gui L., Viviani C., Armato U., Dal Prà I.* (2023) NLRP3 inflammasome's activation in acute and chronic brain diseases — An update on pathogenetic mechanisms and therapeutic perspectives with respect to other inflammasomes. Biomedicines, **11**(4), 999. DOI: 10.3390/biomedicines11040999
39. *de Zoete M.R., Palm N.W., Zhu S., Flavell R.A.* (2014) Inflammasomes. Cold Spring Harb. Perspect. Biol., **6**(12), a016287. DOI: 10.1101/cshperspect.a016287
40. *Guo H., Callaway J.B., Ting J.P.-Y.* (2015) Inflammasomes: Mechanism of action, role in disease, and therapeutics. Nat. Med., **21**(7), 677–687. DOI: 10.1038/nm.3893
41. *Lara-Reyna S., Caseley E.A., Topping J., Rodrigues F., Jimenez Macias J., Lawler S.E., McDermott M.F.* (2022) Inflammasome activation: From molecular mechanisms to autoinflammation. Clin. Transl. Immunology, **11**, e1404. DOI: 10.1002/cti2.1404
42. *Tsuchiya K.* (2020) Inflammasome-associated cell death: Pyroptosis, apoptosis, and physiological implications. Microbiol. Immunol., **64**(4), 252–269. DOI: 10.1111/1348-0421.12771
43. *Sena-dos-Santos C., Braga-da-Silva C., Marques D., Azevedo dos Santos Pinheiro J., Ribeiro-dos-Santos Â., Cavalcante G.C.* (2021) Unraveling cell death pathways during malaria infection: what do we know so far? Cells, **10**(2), 479. DOI: 10.3390/cells10020479

Received: 01. 10. 2024.
Revised: 25. 11. 2024.
Accepted: 28. 11. 2024.

ВЛИЯНИЕ ГОРЬКОГО МЁДА НА ИНФЛАММАСОМ-ЗАВИСИМУЮ ГИБЕЛЬ КЛЕТОК ПРИ ЦЕРЕБРАЛЬНОЙ МАЛЯРИИ: ОЦЕНКА НА ОСНОВЕ СЕТЕВОЙ ФАРМАКОЛОГИИ

М.О. Даниян[1]*, О.Б. Адеое[2], Э. Осирим[1,3], И.Д. Асиянбола[1,4]

[1]Faculty of Pharmacy, Obafemi Awolowo University,
Ile-Ife, Osun State, Nigeria; *e-mail: mdaniyan@oauife.edu.ng
[2]Benjamin Carson (Snr.) School of Basic Medical Sciences, Babcock University, Ilishan-Remo, Ogun State, Nigeria
[3]Faculty of Basic Medical Science, Redeemer's University, Ede, Osun State, Nigeria
[4]College of Health Sciences, Osun State University, Osogbo, Osun State, Nigeria

Церебральная малярия (ЦМ) — смертельно опасное осложнение инфекции, вызванной *Plasmodium falciparum*. Биологическая и физиологическая связь между ЦМ, воспалением и формированием инфламмасом свидетельствует о сложности патологического процесса. Возникновение резистентности к доступным недорогим лекарственным препаратам и усугубляющийся экономический кризис обуславливают необходимость поиска новой эффективной фармакотерапии на основе интеграции подходов официальной и традиционной медицины. Ранее мы изучили лечебные свойства горького мёда и определили его ботанические и биологически активные характеристики, включая ингибирование активности панкреатической альфа-амилазы, антидислипидемические, кардиопротекторные эффекты, а также регенерирующее действие при гепаторенальном синдроме у крыс с диабетом, индуцированным стрептозотоцином. В настоящем исследовании с помощью газовой хроматографии в сочетании с масс-спектрометрией (ГХ-МС) были определены фитохимические соединения горького мёда (ГМ), с использованием диаграмм Венна были обнаружены 9 мишеней среди генов, связанных с ЦМ, воспалением, инфламмасомами и фитокомпонентами ГМ. Сетевой анализ выявил значимые функциональные и физические взаимодействия между белками-мишенями, кодируемыми этими генами, и белками, содержащими NOD- и LRR-домены, а также содержащим пириновый домен белком 3 (NLRP3). Молекулярный докинг фитокомпонентов горького мёда к этим мишеням позволил определить три наиболее перспективных соединения для дальнейшей экспериментальной проверки. На основе полученных данных можно предполагать, что горький мёд может способствовать подавлению инфламмасом-зависимой гибели клеток при ЦМ благодаря взаимодействию с установленными в результате исследования мишенями.

Полный текст статьи на русском языке доступен на сайте журнала (http://pbmc.ibmc.msk.ru).

Ключевые слова: церебральная малярия; воспаление; инфламмасома; горький мёд; фитокомпоненты; сетевая фармакология

Финансирование. Данное исследование не получило ни одного гранта от организаций государственного, коммерческого или некоммерческого сектора.

Поступила в редакцию: 01.10.2024; после доработки: 25.11.2024; принята к печати: 28.11.2024.